J Mater Sci (2008) 43:2833–2843
DOI 10.1007/s10853-008-2526-0

Viscoelasticity of multi-layer textile reinforced polymer composites used in soccer balls

D. S. Price · R. Jones · A. R. Harland · V. V. Silberschmidt

Received: 6 December 2007 / Accepted: 1 February 2008 / Published online: 28 February 2008

Abstract This paper gives details of a comprehensive dynamic mechanical analysis (DMA) material characterisation activity for all constituent layers of two modern-day thermoformed soccer balls. The resulting material data were used to define a series of viscoelastic finite element (FE) models of each ball design which incorporated the through-thickness composite material properties, including an internal latex bladder, woven fabric-based carcass and polymer based outer panels. The developed FE modelling methodology was found to accurately describe the viscoelastic kinetic energy loss characteristics apparent throughout a soccer ball impact at velocities which are typical of those experienced throughout play. The models have been validated by means of experimental impact testing under dynamic loading conditions. It was found that the viscoelastic material properties of the outer panels significantly affected ball impact characteristics, with outer panel materials exhibiting higher levels of viscous damping resulting in higher losses of kinetic energy.

Introduction

The spaghetti analogy used to describe the molecular structure of rubber-like materials [1] defines their inherent viscoelastic properties linked to relative motions of large molecules in the process of deformation. If exposed to constant stress (i.e. creep conditions), rubbers can experience flow, and when subjected to constant strain, will experience non-zero levels of stress. Both phenomena are rate-relaxation and time-dependent viscoelastic effects. Similarly, the complex entanglement of long-chained molecules also gives rise to difficulties with respect to realignment and intermolecular friction throughout rapid straining and so resulting in strain-rate sensitivity and significant stiffening effects when the material is subjected to high strain rates [2]. The measurement of material viscoelasticity is crucial for the determination of material properties under both quasi-static and dynamic events, such as impact. The modern-day soccer ball is an example of a hollow pressurised structure which undergoes multiple impacts, approximately 2,000 impacts per game, and should be designed to withstand these loads whilst exhibiting high levels of performance consistency and uniformity. To engineer soccer balls effectively equipment manufacturers need to understand the mechanical impact characteristics of balls under dynamic loading conditions that are representative of play. This paper details the development of an advanced viscoelastic FE model of the soccer ball validated by a comprehensive dynamic test programme. This is to enable kinetic energy loss impact properties to be characterised by experimentally determined material parameters as opposed to using an external damping co-efficient to tune the model to enable agreement with impact test data. This study therefore provides the first steps in developing a predictive modelling capacity enabling a greater understanding of the effects of material selection on impact characteristics.

D. S. Price (✉) · R. Jones · A. R. Harland · V. V. Silberschmidt
Sports Technology Research Group, Wolfson School of Mechanical and Manufacturing Engineering, Loughborough University, Leicestershire LE11 3TU, UK
e-mail: d.s.price@lboro.ac.uk

Soccer ball material mechanics

Kinetic energy loss

The impact characteristics of sport balls have been investigated by a number of authors covering a wide number of

sports, which employ both hollow pressurised deformable balls such as soccer and tennis [3], and solid deformable balls such as cricket and baseball [4]. A solid ball contains material occupying the entire internal volume of the sphere; a hollow ball is constructed from a spherical shell with a specific wall thickness. Two main types of mechanical models—rigid and deformable—are used for different types of balls in various approaches. Mechanical models of rigid solid and hollow balls of the same diameter differ only in their dynamic parameters due to variations in the distribution of mass. Deformable hollow balls—in contrast to solid ones—can be additionally stiffened by internal pressure. This can be achieved either by means of ball inflation, i.e. in soccer balls, by introducing air into the cavity using a pump device, or in the case of tennis balls by carrying out a controlled reaction, which produces gas inside the spherical shell throughout the manufacturing stages. The effects of internal ball pressure on impact characteristics have been investigated by a number of authors. Armstrong et al. [5] revealed that an increase in pressure caused a stiffer global ball response therefore resulting in higher values of co-efficient of restitution (COR)—the ratio of rebound to inbound velocity, which provides a measurable dynamic metric for the quantification of kinetic energy loss. The air that is used to pressurise the soccer ball obeys the ideal gas law, which is expressed as

$$\tilde{p} = \rho \tilde{R} T = p + p_{\mathrm{A}}, \tag{1}$$

where $\tilde{p}$ is absolute (total) pressure, $\tilde{R}$ is the gas constant, T is the current temperature in Kelvin, p is gauge pressure, p_{A} is atmospheric pressure and ρ is fluid density.

Bridge [6] quantified the adiabatic increase in pressure due to volumetric changes of the ball throughout impact and likened its effect to that of a spring with minimal damping. Hubbard and Stronge [7] found that the effects of internal air pressure become significantly reduced with the increase in the shell's stiffness as apparent in table tennis balls. It was found that COR for soccer balls has a stronger dependence on ball construction than on its internal pressure [8].

The fundamental metrics in the analysis of sports ball impacts include the impact contact time, deformation and COR. It has been shown that COR is dependent upon the global ball stiffness, which in turn depends on both material stiffness and internal pressure [5–7]. The effects of kinetic energy loss made evident through COR manifest themselves through a number of mechanisms. These include: the energy used in the formation and damping of post impact surface waves and modes of vibration [9, 10], plastic deformation [11] and, most significantly, viscoelastic material behaviour [12, 13].

The use of FE models for ball impact modelling has been undertaken previously by Asai et al. [14], Hocknell, [15], Mase and Kersten [16] and Cordingley [17]. Asai et al. developed an FE model of a foot and calf assembly and soccer impact scenario. The model was validated through high speed video (HSV) analysis of maximum velocity instep kicks performed by a number of male soccer players. Details of the soccer ball materials were not provided. Hocknell developed an FE model of the golf club head/ball impact which was validated through the determination of club head mode shapes measured through the combined use of laser vibrometry and electronic speckle pattern interferometry (ESPI). Mase and Kersten describe the use of a dynamic mechanical analyser (DMA) to ascertain viscoelastic properties of golf ball materials as input for FE studies. The golf ball construction in the studys of both Hocknell and Mase and Kersten is based on a two-piece ball with a large polybutadiene core surrounded by an ethylene ionomer cover. Cordingley developed an FE model of a tennis ball validated though normal and oblique impact testing. The ball construction of the tennis ball considered in this study consists of a rubber compound consisting of a mixture of natural rubber, reinforcing fillers, clay, zinc oxide, sulphur and accelerators for the curative system. The outer cloth covering consists of a mixture of natural and synthetic wool-based yarn.

Hocknell, Asai et al. and Cordingley prescribed stiffness proportional damping which is in the form of

$$\sigma_{\mathrm{d}} = \beta D^{\mathrm{el}} \dot{\varepsilon}, \tag{2}$$

where σ_{d} is a damping stress, β is stiffness-proportional Rayleigh damping co-efficient, D^{el} is an elastic modulus in the material's strain-free state and $\dot{\varepsilon}$ is a strain rate.

Stiffness proportional damping, β, and mass proportional damping, α, are related to one another by Rayleigh damping which is the fraction of critical damping ξ_i in the form:

$$\xi_i = \frac{\alpha}{2\omega_i} + \frac{\beta\omega_i}{2}, \tag{3}$$

where for a given mode, i, α is mass-proportional Rayleigh damping and β is stiffness-proportional Rayleigh damping, and ω_i is the frequency at the mode of interest.

Equation 3 does not describe a viscoelastic material; it is used to introduce damping linked to the effects of the stiffness and mass. α-Damping introduces forces caused by the absolute velocities of the model and simulates the structure moving through viscous "ether" (a permeating still fluid so that any motion of any point in the model causes damping) [18]. α-Damping is most effectively used to damp out the low frequency response of the system. β-Damping provides resistive damping stresses at each point within the model that are proportional to the material stiffness and strain rate in accordance with Eq. 2.

The main problem with applying damping co-efficients is that they cannot be physically determined directly and are often used in numerical simulations as a fitting parameter to enable model agreement with experimental results. To develop accurate soccer ball FE models there is a distinct need to determine viscoelastic material properties experimentally to enable direct input into the model to allow for sufficient modelling accuracy to depict kinetic energy loss characteristics.

Theory of linear viscoelasticity

The molecular structure of rubber-like materials results in their specific response to external forces that is between an elastic solid that obeys Hooke's law, and a viscous liquid that obeys Newton's law. Therefore, as with other materials of biological origin [19] rubber-like materials exhibit material viscoelasticity. The basic constitutive equation for linear viscoelasticity for a sample of rubber-like material undergoing simple shear is:

$$\tau(t) = \int_{-\infty}^{t} G(t-s)\dot{\gamma}(s)\mathrm{d}s, \tag{4}$$

where $\tau(t)$ is a shear stress as a function of time, $G(t)$ is a relaxation modulus, $\dot{\gamma}$ is a shear strain rate. The integration is carried out over preceding time steps s, up to the current time t.

The frequency-dependent version of the stress relaxation modulus is the complex modulus, which has greater relevance to a soccer ball impact since it represents material viscoelasticity under dynamic conditions. The complex modulus is determined through the application of sinusoidally varying strain as shown in Fig. 1.

The complex modulus G^* has two components:

$$G^* = G' + iG'', \tag{5}$$

a storage modulus G', which contributes to the stress that is in phase with the imposed strain (Fig. 1a), and a loss modulus G'', which contributes to the stress that is 90° out of phase with the imposed strain (Fig. 1b). G' specifies the energy stored in the specimen due to the applied strain and G'' specifies the dissipation of energy as heat [20].

The magnitude of both loss and storage moduli determine the magnitude of the phase difference δ between the total stress and the imposed strain, as shown in Fig. 1d. The phase difference δ indicates the extent of material's viscosity, with $\delta = 0°$ and $\delta = 90°$ being equivalent to perfectly elastic and perfectly viscous materials, respectively. A further parameter is the loss factor η, which provides a measure of material's damping and is defined as:

$$\eta = \frac{G''}{G'} = \tan\delta, \tag{6}$$

Figure 2 gives details of two characteristic responses of G', G'' and $\tan\delta$ with frequency for a typical styrene butadiene rubber. At low frequencies G' can be considered fairly constant, however G'' increases with an increase in frequency at a greater rate than G'. This can be explained by specific features of the molecular microstructure. At low frequency slowly moving polymer chain segments can change their configurations in accordance with the induced strain, resulting in $G' > G''$. At higher frequencies, however,

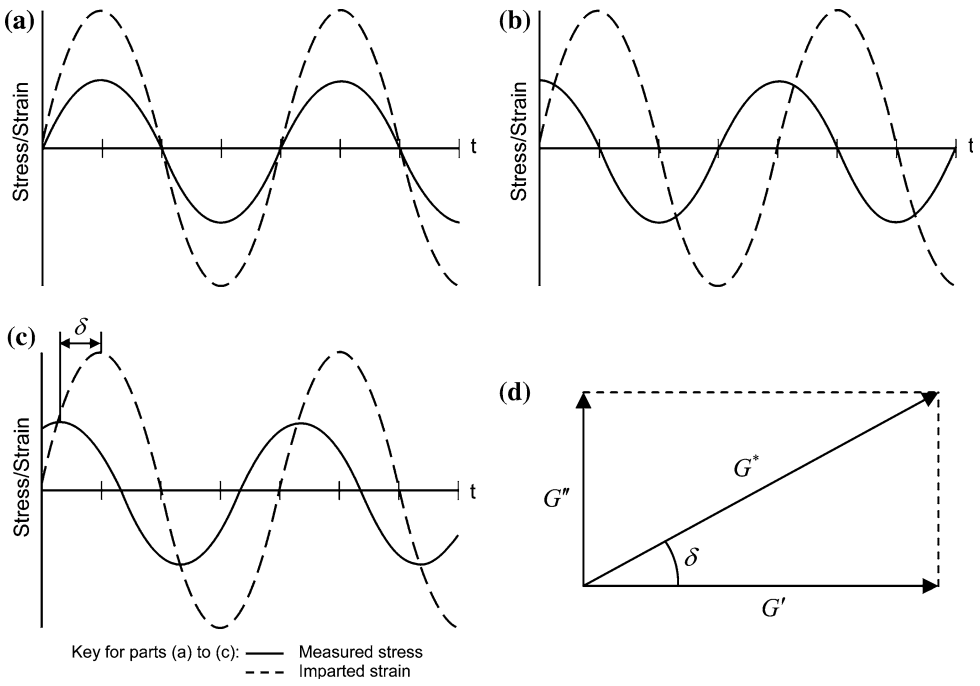

Fig. 1 Cyclic stress strain diagrams for (**a**) elastic, (**b**) viscous and (**c**) viscoelastic materials, (**d**) complex modulus diagram for viscoelastic material

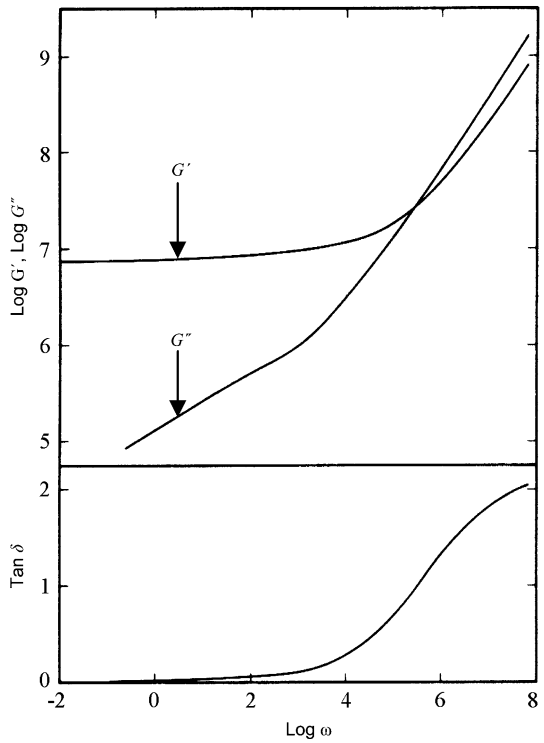

Fig. 2 Plot of log G', log G'' and tan δ against angular frequency for a typical viscoelastic material adapted from Mark et al. [15]

there is less time for configuration changes resulting in considerable part of deformation energy being dissipated as heat, due to the increased friction generated at entanglement sites. This results in $G'' > G'$ and a higher level of the loss factor, which increases with increasing frequency [21], as shown in Fig. 2. It should also be noted that Fig. 2 only represents one class of material. The shape of the curves shown in Fig. 2 depends upon the chemical nature of the material, and some rubbery materials and foams do not experience an increase in G', G'' and η with frequency.

Measurement of viscoelastic properties

The techniques involved in the measurement of G', G'' and η are dependent upon the frequency range of interest [22–25], and generally there are five methods of measurement including: creep and stress relaxation, torsion pendulum, forced vibration non-resonance, resonance and wave propagation methods. The dynamic mechanical analysis (DMA) is a forced vibration technique that allows for the measurement of viscoelastic behaviour in the frequency range 0.1–1,000 Hz, and typically involves the simultaneous application of strain and the measurement of total stress as described by Read and Dean [26]. Given the contact time for a soccer ball impact with an inbound velocity ranging from 7 to 31 ms^{-1} lasts between 7 and 10 ms, it is necessary to measure viscoelastic properties at a range of frequencies. This makes DMA a suitable technique to determine viscoelastic properties of a soccer ball material.

Soccer ball construction

Two modern ball construction types, ball A and B (Fig. 3), were considered in this study, and their exact material details

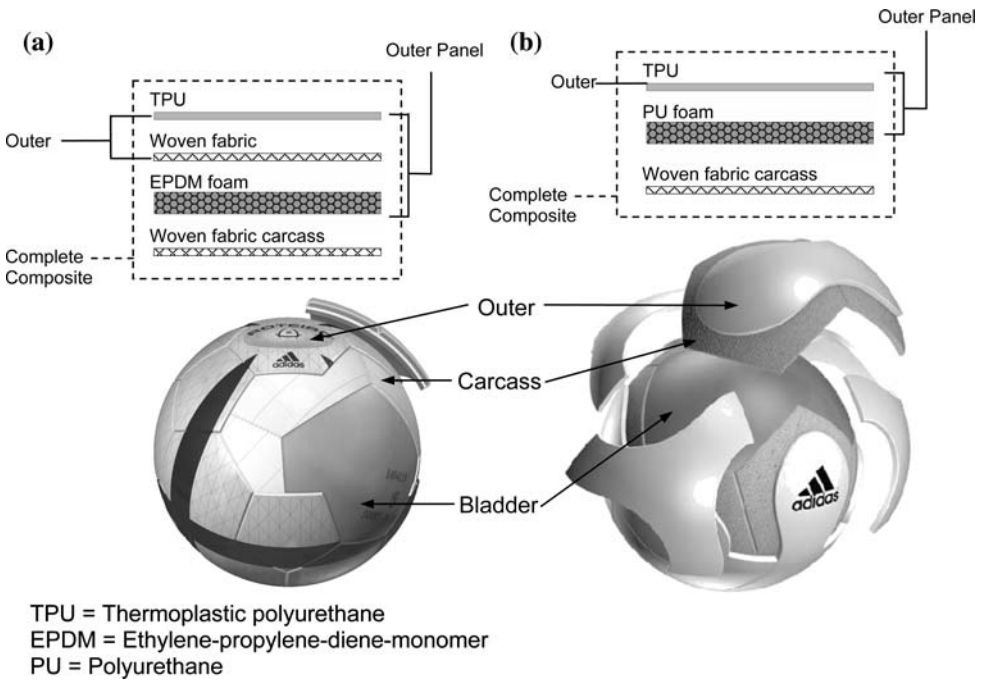

Fig. 3 (**a**) Ball A and (**b**) ball B construction details

are regarded as the industrial partner's proprietary. Both balls utilise a machine-stitched 12-panel dodecahedron underling carcass, with thermally bonded multi-layer composite outer panels, pressurised by an internal natural rubber latex bladder. The carcass material consists of two polyester yarn-based plain-woven fabric layers bonded together by natural rubber latex glue. The outer panel designs are based on a foam and outer layer arrangement. The outer layer in ball A consists of an Ethylene-propylene-diene-monomer (EPDM) foam, a woven fabric layer, and a thermoplastic polyurethane (TPU) outer layer bonded together by natural rubber latex. Ball B consist of a polyurethane (PU) foam and a TPU outer skin layer only.

DMA tests

Experimentation system

A TA Instruments 2890 DMA system was used to determine viscoelastic properties of the individual constituent material layers, the outer layer and the complete composite material as defined in Fig. 3 for ball types A and B. Measurements of storage and loss moduli were carried out at a frequency range of 0.1—100 Hz. Although this range does not cover oscillations with higher frequencies during the impact, the major losses are linked with lower ones which are covered by measurement range used throughout this study. Tensile DMA testing was implemented for all constituent material layers. The material test specimens extracted from ball types A and B were 40 mm × 5 mm in length and width, with the thickness being equal to the layer thickness, ranging from approximately 0.5 to 3 mm. All tests were conducted at ambient room temperature, 23 °C, and due to the maximum allowable force amplitude of the machine being 18 N, a displacement amplitude of 20 μm was used. The effects of material orientation were also considered in specimens that contained fabric with the tensile test pieces being tested along the yarn direction (0°) and along the bias direction (45°). Figures 4–6 summarise details of DMA test results; data for storage modulus, loss modulus and loss factor are presented with respect to frequency, with each curve showing an average of two specimens.

Results

The individual layer's contributions for ball types A and B (Figs. 4 and 5) show a wide range of elastic and storage moduli data which reflect the diverse range of constituent material layers used to form the complete composite material. The results are consistent with the theory presented in Sect. 'Soccer ball material mechanics': a greater rate of change as frequency is increased is apparent in the

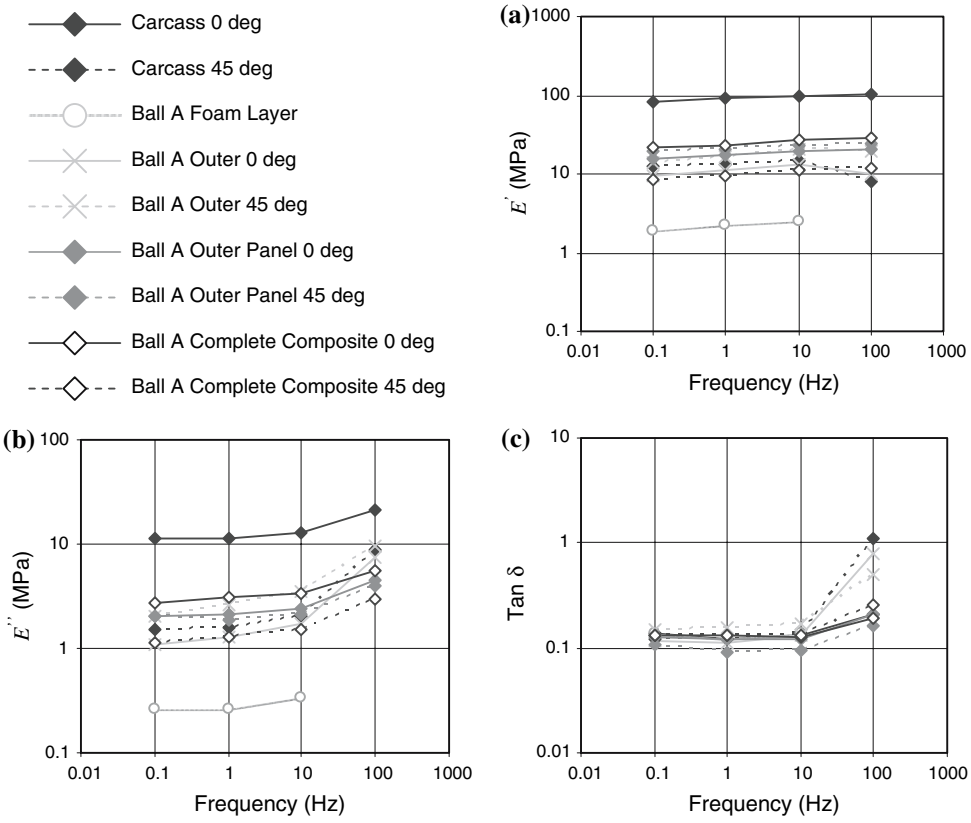

Fig. 4 Viscoelastic properties of ball A constituent layers: (**a**) storage modulus, (**b**) loss modulus and (**c**) tan δ

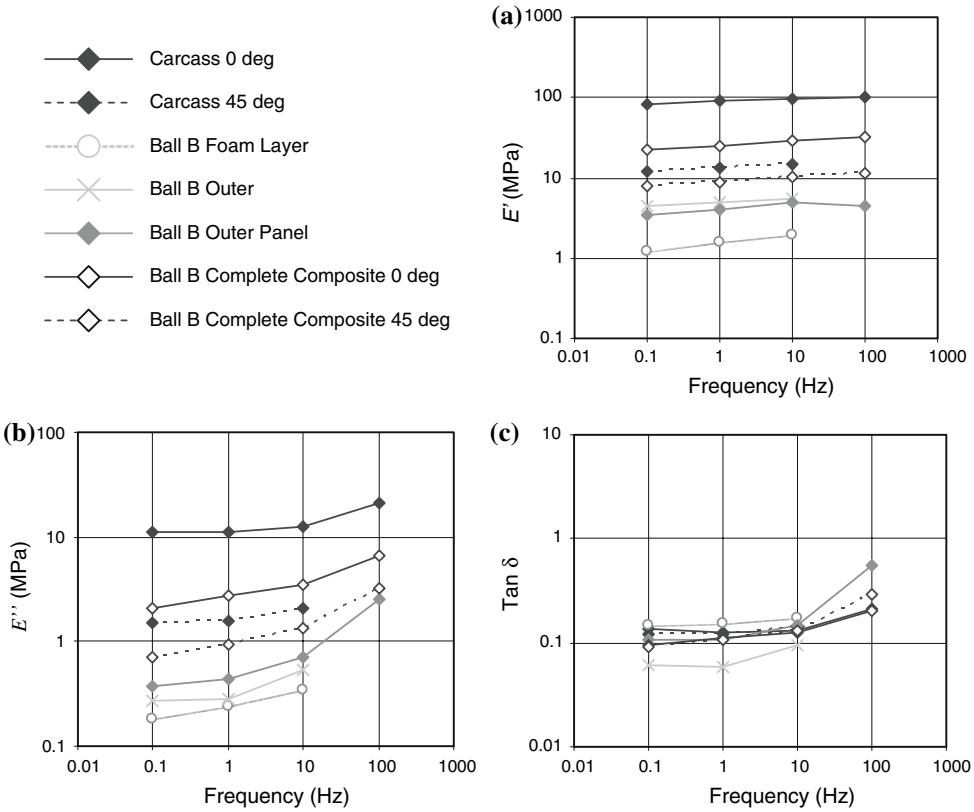

Fig. 5 Viscoelastic properties of ball B constituent layers: (**a**) storage modulus, (**b**) loss modulus and (**c**) tan δ

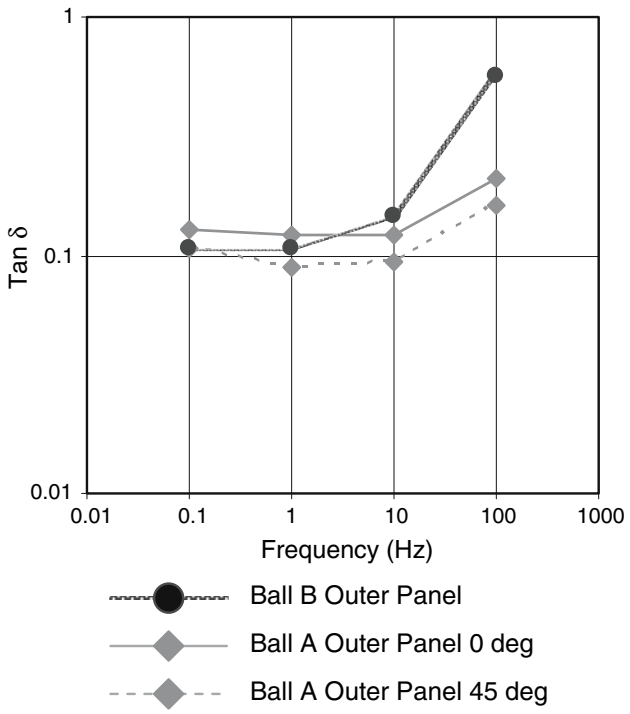

Fig. 6 Damping properties of ball A and B outer panel materials

loss modulus when compared to the storage one. It was also shown in Sect. 'Soccer ball material mechanics' that tan δ increases with frequency; this feature is confirmed for the studied materials. It was found that the foam layer exhibited higher levels of material damping (Fig. 5b) than the other constituent layers, which is consistent with a notion of foam materials being conventionally developed to have good vibration isolation and damping characteristics.

From analysis of data for 0° in Figs. 4 and 5 it follows that irrespective of the higher levels of damping associated with the outer panel and foam layers, the complete composite material demonstrates similar tan δ to that of the carcass material. This provides evidence that the carcass layer when strained at 0° dominates the damping properties of the entire composite material. A similar trend is observed for the storage modulus for the carcass strained at 0°, which is significantly stiffer than all other constituent materials. This indicates the significant effects of material anisotropy to be significant, which was also found in a previous study by Price [27]. It is also shown that the complete composite material exhibits damping properties that are different to that of the carcass strained at 45°, indicating the effect of other constituent materials on the deformation behaviour along the bias.

Figure 6 compares viscoelastic material data for the outer panel material for both ball types and demonstrates that ball B exhibits higher levels of material viscoelasticity than ball A.

The DMA study revealed that materials used for ball construction behave in a viscoelastic manner, indicated by variations of storage and loss moduli, and tan δ with

frequency. The results have also revealed an anisotropic viscous behaviour in the form of direction-dependent material damping properties. The main finding of the DMA testing indicates significantly higher levels of material damping associated with the outer panel material in ball B, when compared to ball A.

Implementation of DMA data into finite element simulations

FE numerical simulations were implemented with the use of the Abaqus EXPLICIT software package. Material viscoelasticity was introduced into the software by utilising Eq. 4 and by using a dimensionless relaxation modulus $g(t)$, as opposed to $G(t)$. This is carried out by the formation of a Prony series by the software, which is based upon exponential functions describing the stress relaxation modulus $g(t)$. Significantly easier integration of Eq. 4 allows for adequate definition of material viscoelasticity. The software makes use of Fourier transform to allow storage and loss moduli data to be converted into a Prony series [28]. This is achieved by supplying real and imaginary parts of the Fourier transform of the non-dimensional shear relaxation function $g^*(\omega)$ alongside their respective frequencies as follows:

$$Re[g^*(\omega)] = G''/G_\infty, \tag{7}$$

$$Im[g^*(\omega*)] = 1 - \ G'/G_\infty, \tag{8}$$

where G_∞ is the long-term shear modulus, which was derived from the quasi-static tensile tests.

As all materials used in the ball are considered isotropic, their Poison's ratio v, shear and elastic moduli are related by

$$G = \frac{E}{2(1+v)}. \tag{9}$$

It follows that:

$$Re[g^*(\omega)] = G''/G_\infty = \ E''/E_\infty, \tag{10}$$

$$Im[g^*(\omega*)] = 1 - \ G'/G_\infty = 1 - \ E'/E_\infty, \tag{11}$$

Therefore the necessary data were derived from the elastic modulus based DMA data. This in turn enabled the formation of the Prony series and to characterise the viscoelastic material properties of the soccer ball materials.

The DMA data were used to characterise the viscoelastic material properties of three soccer ball FE models, as shown in Fig. 7. Each model utilised linear-interpolation composite shell elements to allow a through-thickness composite structure of the panels to be sufficiently modelled. This modelling methodology was in part adopted due to the success seen in previous studies concerning computational modelling of fabric materials, [29]–[32]. Pressurisation of each model was permitted through an integral layer of hydrostatic fluid elements, which share the nodes of the structural shell elements. The fluid elements were coupled with a cavity reference node, which possessed a single degree of freedom to represent the pressure of the cavity. A mass flow rate was applied to the cavity reference node, which simulated the flow of a pneumatic compressible fluid within the cavity, to represent the air within the bladder and allow for pressurisation. The pneumatic fluid behaves like an ideal gas as detailed in Eq. 1 and allows the uniform increase in cavity pressure throughout impact to be properly modelled. Based on previous studies as detailed in Sect. 'Kinetic energy loss' the air was assumed to act as a spring with minimal damping, and the effects of outer panel materials were considered to be more significant. FE model 1 is a basic

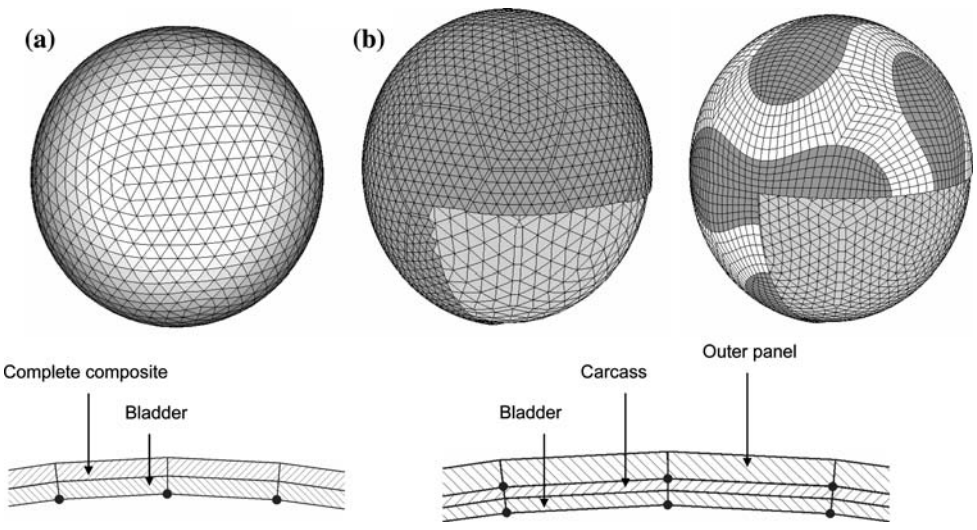

Fig. 7 (**a**) FE model 1 and (**b**) FE models 2 and 3

model of the ball type A with the ball structure based on an icosahedron allowing for a uniform arrangement of triangular shell elements to be adopted. FE models 2 and 3 are advanced FE models of ball types A and B and include an accurate representation of the respective outer panel designs as detailed in Fig. 7.

The material stiffness characteristics of ball types A and B were determined through a series of quasi-static uniaxial tensile tests using a standard tensile test machine. These were performed on dumbbell specimens of the constituent layers, outer panels and complete composite material layers conforming to BS 903 Part A2 [33]. A hyperelastic reduced polynomial strain energy potential equation was calibrated against the material data, through a least squares fit procedure. This procedure was carried out by the FE software and allowed for the characterisation of the ball materials.

FE model validation

A series of impact tests were carried out on ball types A and B to enable FE model validation. Each impact was carried out using a bespoke 2-wheel ball launch device, which introduced the ball between two counter-rotating rollers launching it at the required velocity onto a steel plate 2 m away. These tests included impacting five balls of each type, five impacts for each ball along the direction orthogonal to the plane of the steel plate which acted as a target. Impacts occurred at inbound velocities of 9 (representative of a standard drop test), 14, 22 and 32 ms^{-1}. Ball motion and impact were recorded using a Photron Fastcam—Ultima APX 120 K HSV camera operating at 10,000 frames per second, which was remotely triggered to initiate the storage of images into a microprocessor linked to a laptop through a firewire connection. Each audio video interleave (AVI) file was imported into Image Pro Plus (IPP), a 2D image analysis software package, which allowed for the determination of impact contact time, longitudinal and tangential deformation, velocity and COR.

Implementation of FE ball models

The DMA data for the bladder and complete composite material were used to characterise material properties for FE model 1, the basic FE model for ball type A. In numerical simulations the ball model was impacted against a rigid surface that was constrained with regard to all degrees of freedom. Numerical simulations were performed for four levels of the inbound speed, used in experiments. Figure 8 provides data for COR, deformation and contact time.

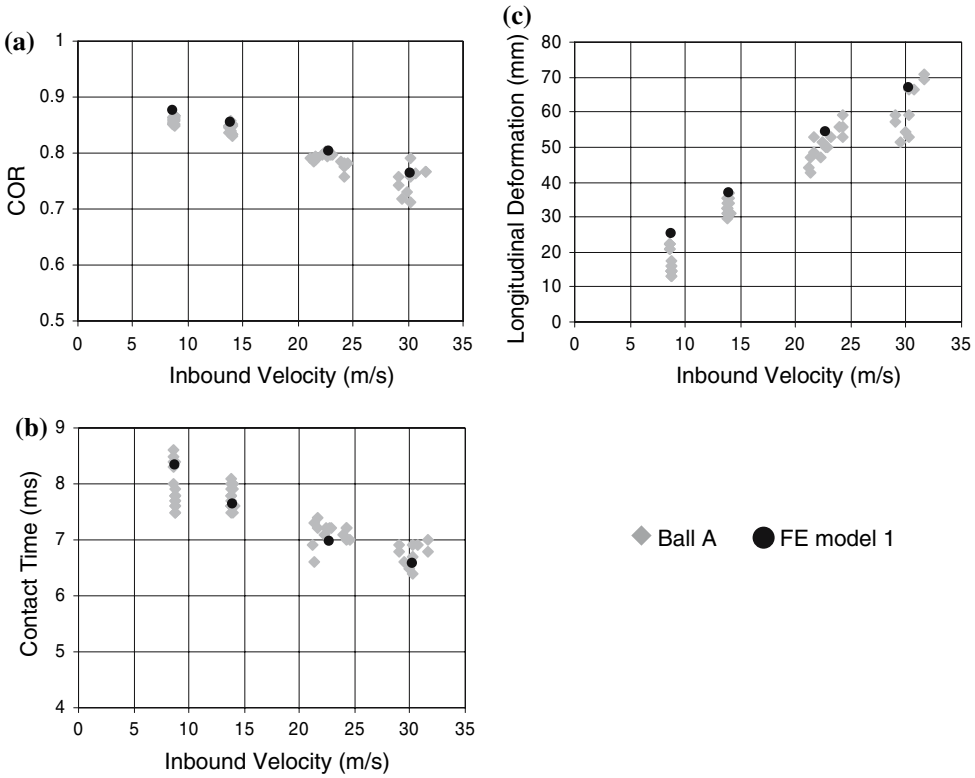

Fig. 8 Impact data for ball type A—experiment results and numerical simulation data for model 1: (**a**) COR, (**b**) contact time, (**c**) longitudinal deformation

The agreement reached between experimental and model COR data as featured in Fig. 8a is within 2% of experimental averages. It should also be noted that the hyperelastic material model used to define the elastic response in FE model 1 was based upon tensile testing carried out at low deformation rates (1,000 mm/min). However agreement is also apparent between the experimental and numerical results for the contact time and deformation as detailed in Fig. 8b and c. This indicates that the viscoelastic material model includes the effects of strain-rate sensitivity—as detailed in Sect. 'Theory of linear viscoelasticity'—that for a given material results in a stiffer response at high strain rates. The viscoelastic material model accounts for these effects by formulating the material response based on the experimental data on the increase of the storage modulus with frequency presented in Sect. 'DMA tests'.

DMA data for the bladder, carcass and respective outer panels for ball types A and B were used to define the viscoelastic behaviour of FE ball models 2 and 3. In simulations each ball model was impacted against a rigid surface at the four prescribed velocities.

As shown in Fig. 9a there are clear differences in both the levels of COR, and the relationship between COR and inbound velocity between both ball types. Ball type A gives higher levels of COR, indicating lower levels of kinetic energy loss throughout impact, when compared to ball type B. The COR data detailed in Fig. 9a give agreement between FE model 2 and the averaged experimental results for ball type A to be within 1.2% for ball type B it is within 3%. The developed viscoelastic FE models predict COR levels as a function of the disparate material damping properties of both ball types, with good agreement with experimental data. The difference in the decline of COR with the inbound velocity for two balls is reproduced by the models. This indicates the importance of the outer panel material used within the new generation ball types as a principal energy loss mechanism.

Figure 9b and c give details of dependences of contact time and longitudinal deformation on the impact velocity and reveals differences between both ball types. Ball type A is characterised by lower contact times, and lower levels of deformation than ball type B indicating a stiffer response. These trends are properly reflected by the models; however there is a slight underestimation of the contact time for FE model 2 and ball type A resulting in a 10% difference between model and experimental results. Figure 10 vividly demonstrates that FE simulations adequately reproduce deformation processes for ball type B during it interaction with the target observed in experiments.

Figure 11 gives details of stress levels developed within the outer panels of FE model 3 which is compared against an earlier version of the model that incorporated a

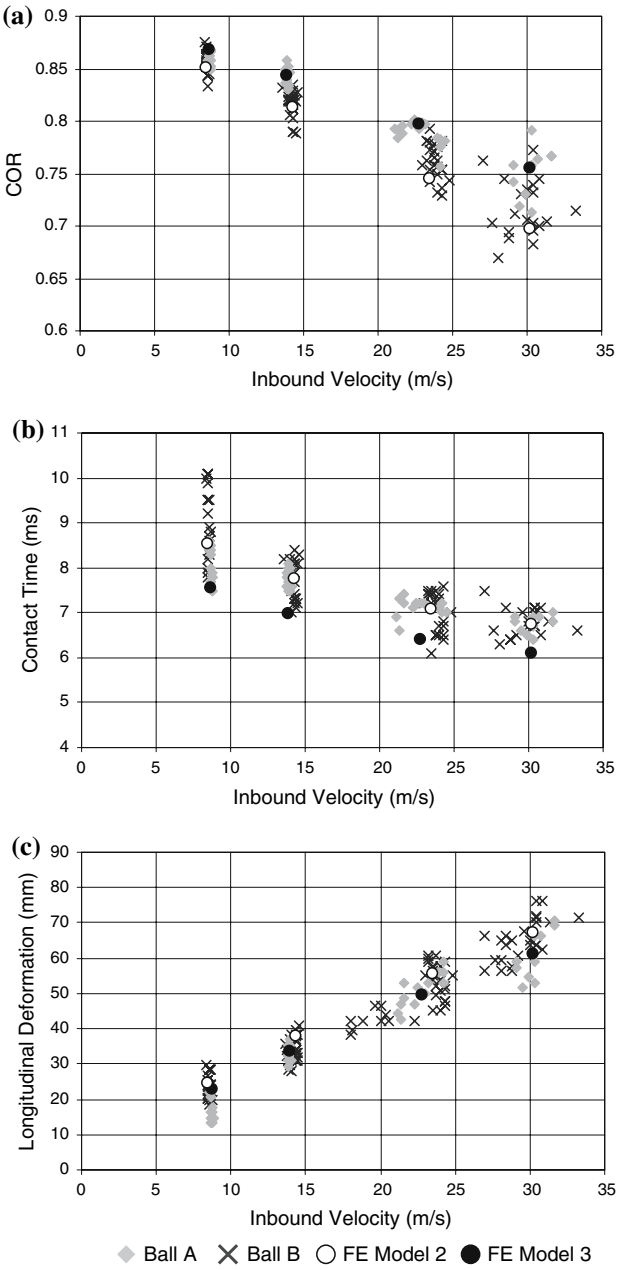

Fig. 9 Experimental and numerical results following: impacts of ball types A and B. (**a**) COR, (**b**) contact time and (**c**) longitudinal deformation

β-damping co-efficient. The viscoelastic version of FE model 3 exhibits greater levels of outer panel stress for the same inbound velocity. This can be linked to the strain—rate sensitivity in the material model (see Sect. 'Theory of linear viscoelasticity'). The FE models of soccer balls developed in this study were found to adequately replicate the deformation and kinetic energy loss characteristics exhibited by thermoformed ball designs used in elite competition.

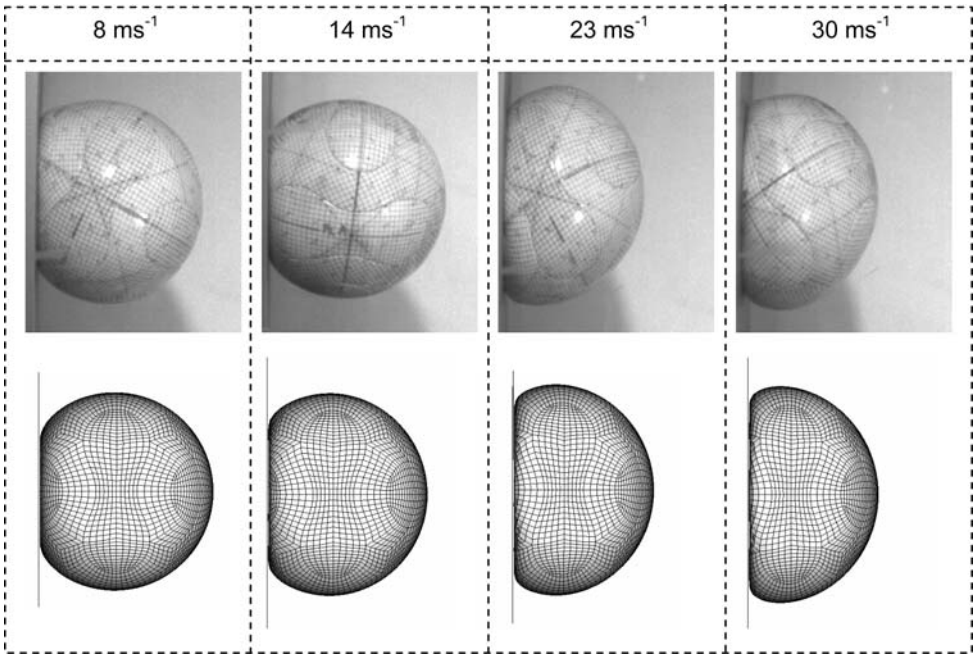

Fig. 10 Impact data for ball B and respective FE model at the moment of maximum longitudinal contraction

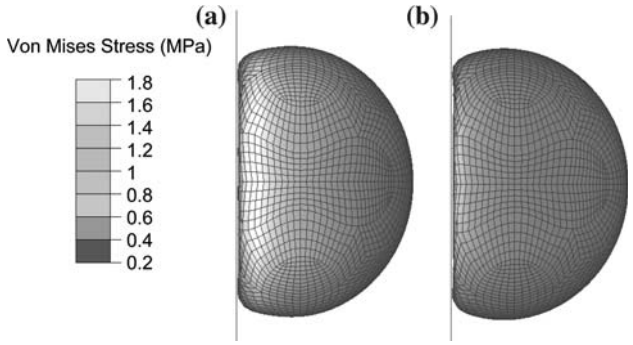

Fig. 11 Effect of strain-rate sensitivity on stresses in outer panel (**a**) viscoelastic FE model 3 (**b**) artificially damped FE model 3

Conclusions

This paper demonstrates that DMA tests on constituent materials can produce data to characterise material viscoelasticity of the composite balls and, hence, to enable accurate estimation of the kinetic energy loss exhibited by soccer balls under impact loading. This has been demonstrated for a range of FE models based on direct introduction of several material layers. Experimental results demonstrated a wide range of damping properties of layers with high levels of damping for foam materials when compared to the other constituent layers. This study also revealed anisotropic material viscoelasticity, with greater levels of damping found in testing fabric-based materials along the material bias, as compared to along their yarn directions.

The use of viscoelastic material data obtained with DMA has revealed the relationship between viscoelasticity of the outer panel material and COR magnitudes characteristics, and has allowed the model to differentiate between outer panels that have high tan δ levels and, subsequently, low COR magnitudes (i.e. ball type A). This study has indicated COR to be strongly influenced by material damping and has presented an experimental means of its quantification. It has been shown that the use of DMA data accounts for the effects of strain-rate sensitivity by including the storage modulus data, which were experimentally found to increase with frequency. This study has provided a framework to estimate the kinetic energy loss linked with material viscoelasticity making a basis for an improved understanding of the dynamic properties of soccer balls.

Acknowledgements The authors would like to acknowledge EPSRC, adidas and Abaqus for their support for this project.

References

1. Treloar LG (1949) The physics of rubber elasticity. Oxford University Press, London
2. Baumann JT (1998) A theory of the elastomer stress–strain curve, In: Proceedings of the meeting of the rubber Division American Chemical Society, Nashville, Tennessee, September 1998, p 1
3. Brody H (1990) Phys Teach 28:407
4. Adair RK (1994) The physics of baseball. Harper Collins, New York
5. Armstrong CW, Levendusky TA, Eck JS, Spyropoulos P, Kugler L (1988) Influence of inflation pressure and ball wetness on the impact characteristics of two types of soccer ball, science and football: Proceedings of the first World Congress of Science and Football. In: Reilly T (ed) E & FN Spon, London, p 394
6. Bridge NJ (1998) Phys Educ 33(3):174

7. Hubbard M, Stronge WJ (2001) Sports Eng 4:49
8. Holmes G, Bell MJ (1985) J Sports Turf Res Inst 61:32
9. Bayman BF (1976) Am J Phys 44(7):671
10. Bridge NJ (1998) Phys Educ 33(4):236
11. Falcon E, Laroche C, Fauve S, Coste C (1998) Eur Phys J B 3:45
12. Hendee SP, Greenwald RM, Crisco JJ (1998) J Appl Biomech 14:390
13. Calvit HH (1967) Int J Solids Struct 3:951
14. Asai T, Carre MJ, Akatsuka T, Haake SJ (2002) Sports Eng 5:183
15. Hocknell A (1998) Computational and experimental analysis of elastic deformation in impact. PhD Thesis, Loughborough University, Loughborough, UK
16. Mase T, Kersten AM (2004) Experimental evaluation of a 3-D hyperelastic rate dependant golf ball constitutive model. In: Hubbard M, Mehta RD, Pallis JM (eds) The engineering of sport 5, vol 2, p 238
17. Cordingley L (2002) Advanced modelling of hollow sports ball impacts. PhD Thesis, Loughborough University, Loughborough, UK
18. Abaqus (2003) Abaqus Version 6.4 users manual volume I: introduction, spatial modelling, execution and output. Abaqus INC
19. Amada S, Lakes RS (1997) J Mater Sci 32:2693
20. Ferry JD (1980) Viscoelastic properties of polymers. John Wiley and Sons, Chichester
21. Mark JE, Erman B, Eirich FR (1994) Science and technology of rubber. Academic Press, London
22. Oyadiji SO (2004) How to analyse the static and dynamic response of viscoelastic components. NAFEMS, Bireniehill, Glasgow
23. Wojtowicki JL, Jaouen L, Panneton R (2004) Rev Sci Instrum 75(8):2569
24. Deverge M, Jaouen L (2004) A review of experimental methods for the elastic and damping characteristics of acoustical porous materials, Proceedings of the 33rd international congress and exposition on noise control engineering (inter-noise 2004), Prague, Czech Republic, August 2004, p 1 [CD-ROM]
25. Lagakos N, Jarzynski J, Cole JH, Bucaro JA (1986) J Appl Phys 59(12):4017
26. Read BE, Dean GD (1978) The determination of dynamic properties of polymers and composites. Adam Hilger Ltd., Bristol
27. Price DS, Harland AR, Jones R (2006) Mater Sci Eng A 420:100
28. Abaqus (2003) Abaqus version 6.4 users manual vol III: materials. Abaqus INC
29. Xue P, Xiongqi P, Cao J (2003) Compos Pt A Appl Sci Manuf 34:183
30. Dong L, Lekakou C, Bader MG (2000) Compos Pt A Appl Sci Manuf 31:639
31. Cavallaro PV, Johnson EJ, Sadegh AM (2003) Compos Struct 61:375
32. Tan P, Tong L, Steven GP (1997) Compos Pt A Appl Sci Manuf 28A:903
33. BS 903-A2 (1995) Physical testing of rubber—part A2: methods for determining tensile stress–strain properties